ChemComm

Cite this: *Chem. Commun.*, 2012, **48**, 5307–5309

www.rsc.org/chemcomm

COMMUNICATION

Efficient determination of diffusion coefficients by monitoring transport during recovery delays in NMR†

Rafal Augustyniak,[abc] Fabien Ferrage,*[abc] Christian Damblon,[d] Geoffrey Bodenhausen[abce] and Philippe Pelupessy[abc]

Received 26th January 2012, Accepted 28th March 2012
DOI: 10.1039/c2cc30578j

A novel NMR approach allows one to efficiently determine translational diffusion coefficients of macromolecules in solution. This method for Signal Optimization with Recovery in Diffusion Delays (SORDID) monitors transport occurring during the recovery times between consecutive scans so that the duration of the measurements can be reduced approximately by a factor two.

Nuclear magnetic resonance spectroscopy (NMR) provides a method of choice to probe transport phenomena on a microscopic scale. In liquid phase, it is possible to explore translational displacements of molecules due to diffusion or flow.[1,2] Although diffusion can be determined by other methods, pulsed field gradient (PFG) techniques are not invasive and offer a remarkable degree of detail both *in vitro* and *in vivo*.[3–5] The development of Diffusion Ordered Spectroscopy (DOSY) boosted the interest in diffusion experiments by opening the way to mixtures such as cell extracts and other multi-component systems.[6] The slow diffusion of macromolecules can only be characterized if the memory of the spin system is long enough to allow detectable displacements to occur between encoding and decoding PFGs. The use of heteronuclear stimulated echoes (XSTE)[7–10] or long-lived spin states[11] allows one to extend diffusion intervals and makes it possible to monitor slow diffusion of large macromolecules. New longitudinal and transverse relaxation-enhanced XSTE experiments, which offer improved sensitivity and resolution, have recently been introduced.[12,13] The combination of XSTE with Band-selective Excitation Short-Transient (BEST) techniques proved to be particularly efficient.[12,14]

Here we report a new NMR scheme designed to measure small diffusion coefficients D of ^{13}C or ^{15}N enriched macromolecules. As in XSTE experiments, information about spatial displacements is stored as longitudinal polarization of nuclei with long spin-lattice relaxation times such as ^{13}C or ^{15}N. In the new experiment, the diffusion interval Δ extends over two consecutive scans and includes the recovery delay T_{RD} between the two scans. When Δ and T_{RD} are of comparable length, this experiment allows one to halve the experimental time.

The pulse sequence for the new experiment is shown in Fig. 1. 'Purging' PFGs G_y and G_z eliminate unwanted magnetization components and ensure efficient water suppression. To encode and decode the positions of the molecules before and after displacement, PFGs G_x with a duration δ and variable amplitudes are applied along the x-axis, so as to minimize convection effects. The phase $\varphi(x)$ acquired by the transverse magnetization of the protons at a spatial position x

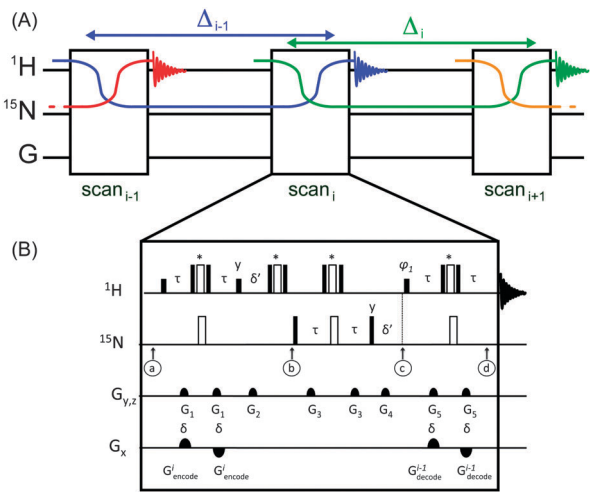

Fig. 1 (A) Principle and (B) details of the pulse sequence for Signal Optimization with Recovery in Diffusion Delays (SORDID), designed for the efficient measurement of slow diffusion coefficients. The diffusion delay Δ extends over two consecutive transients. Filled and open rectangles represent 90° and 180° pulses, respectively. Hard composite pulses[16] $(75°)_{34}(285°)_{144}(75°)_{34}$ are indicated by stars, while lower rectangles represent 90° pulses centred on the amide or imino regions in proteins or RNA, respectively, optimized to cause a 360° rotation of the H_2O magnetization about a tilted field. Unless otherwise specified, all pulses are applied along the x-axis of the rotating frame. The diffusion gradients $G^i_{encode} = G^i_{decode}$ have variable strengths but constant duration δ = 1 ms. The delays are $\tau = |4J_{HN}|^{-1} = 2.72$ ms for $J_{HN} \approx -92$ Hz as in INEPT sequences. The phase cycling employed was $\varphi_1 = x, -x$.

[a] *Ecole Normale Supérieure, Département de Chimie, 24 rue Lhomond, 75231 Paris Cedex 05, France. E-mail: Fabien.Ferrage@ens.fr*
[b] *Université Pierre et Marie Curie, Paris, France*
[c] *UMR 7203 Laboratoire des Biomolécules CNRS-UPMC-ENS, Paris, France*
[d] *Chimie Biologique Structurale, Institut de Chimie, Sart-Tilman (B6c), Université de Liège, 4000 Liège, Belgium*
[e] *Institut des Sciences et Ingénierie Chimiques, BCH, Ecole Polytechnique Fédérale de Lausanne, 1015 Lausanne, Switzerland*
† Electronic supplementary information (ESI) available. See DOI: 10.1039/c2cc30578j

after a bipolar gradient pair is $\varphi(x) = 2\kappa x$, with $\kappa = \gamma s \delta G_{max}$, where γ is the magnetogyric ratio of protons, s the shape factor of the PFGs, and G_{max} their peak amplitude. Note that all gradients can be applied along the z-axis on a single-axis gradient probe,[15] as long as convection along this axis is constrained.

After a few 'dummy' scans, the magnetization of the spin system at point **a** comprises two components: $H_z^{(i)}$ that will serve to encode the spatial position of a molecule during the scan i and $N_z^{(i-1)enc}$, encoded during the previous scan. A sequence for Insensitive Nuclei Enhanced by Polarization Transfer (INEPT)[17] converts these two terms into longitudinal two-spin order $2H_zN_z^{(i)enc}$ and $-N_z^{(i-1)enc}$ that are both spatially modulated with an amplitude cos $\varphi(x)$. Between points **b** and **c** the sequence converts the term $2H_zN_z$ into $-N_z^{(i)enc}$ that will merely be inverted to give non-observable $N_z^{(i)enc}$ during the last INEPT sequence. Meanwhile, the component encoded during the previous scan is converted into $2H_zN_z^{(i-1)enc}$ at point **c** and, finally, transformed by the last INEPT sequence into observable $H_x^{(i-1)dec}$ at point **d**. While this transverse proton magnetization is detected and allowed to relax towards equilibrium, the information about the position of the molecules during scan i is stored as longitudinal nitrogen-15 magnetization $N_z^{(i)enc}$ during the recovery delay T_{RD}. It will be decoded and detected during the following $(i + 1)$th scan. The amplitude of the diffusion gradients must be changed in each scan, i.e., $G^{i-1}_{encode} = G^{i-1}_{decode} \neq G^{i}_{encode} = G^{i}_{decode}$, so that only polarization that has been encoded in the $(i - 1)$th scan is decoded and detected in the ith scan. This ensures that the polarization can be stored as longitudinal nitrogen-15 magnetization during the long diffusion and recovery delays, without requiring any phase cycling of the nitrogen-15 pulses.

The diffusion coefficient can be determined by fitting the experimental data to the usual equation:

$$S/S_0 = \exp(-D4\kappa^2\Delta) \quad (1)$$

where S is the signal integral observed with a gradient intensity G; S_0 is the limit of S when the diffusion gradients have vanishing amplitudes $G = 0$; and Δ is the *total* diffusion delay defined to embrace two consecutive scans, as indicated in Fig. 1, i.e., $\Delta = T_{RD} + 10\tau + 2\delta'$, where the recovery delay T_{RD} is defined as the duration between the beginning of signal acquisition of scan i and the first pulse of scan $i + 1$. The sensitivity of an experiment is proportional to the signal-to-noise ratio per time unit for a vanishing gradient $G = 0$:

$$f_{SORDID} \sim S_0/\sqrt{\Delta} \sim \left\{1 - \exp[-R_1(^1H)\Delta]\right\}\exp[-R_1(^{15}N)\Delta]/\sqrt{\Delta} \quad (2)$$

where $R_1(^1H)$ and $R_1(^{15}N)$ are the average longitudinal relaxation rates of protons and nitrogen-15 nuclei. One may compare this relationship with the signal-to-noise ratio per time unit for the BEST-XSTE experiment, which is more sensitive than the basic XSTE method:[12]

$$f_{BEST\text{-}XSTE} \sim \left\{1 - \exp[-R_1(^1H)T_{RD}]\right\} \times \exp[-R_1(^{15}N)\Delta]/\sqrt{T_{RD} + \Delta} \quad (3)$$

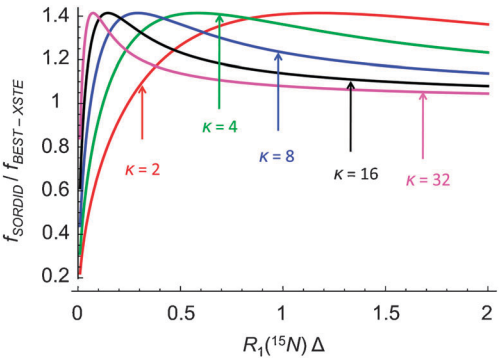

Fig. 2 Theoretical signal gain of SORDID over BEST-XSTE calculated from eqn (2 and 3) for different ratios $\kappa = R_1(^1H)/R_1(^{15}N) = 2$ (red), 4 (green), 8 (blue), 16 (black) and 32 (magenta) corresponding to increasing rotational correlation times. The gains are plotted as a function of the dimensionless product $R_1(^{15}N)\Delta$.

When the recovery and diffusion delays have the same duration $T_{RD} = \Delta$, the sensitivity of the SORDID experiment is $\sqrt{2}$ times better than BEST-XSTE. In practice this allows one to decrease the experimental time by a factor of 2. The best value of Δ for which the highest gain can be obtained depends on the ratio $\kappa = R_1(^1H)/R_1(^{15}N)$.

Theoretical curves representing the gain in sensitivity as a function of the product of the nitrogen-15 longitudinal relaxation rate $R_1(^{15}N)$ and the diffusion delay Δ are shown in Fig. 2. In most cases, SORDID is more efficient than BEST-XSTE, unless very short diffusion delays are used in small proteins. For instance, for a small protein with $\kappa = 4$, the diffusion delay should be $\Delta > 0.12/R_1(^{15}N)$ for SORDID to be more efficient, while for $\kappa = 2$, this delay should be $\Delta > 0.25/R_1(^{15}N)$. For example, for ubiquitin, $\kappa_{ub} = 2.8$ and $0.25/R_1(^{15}N) = 150$ ms, a value shorter than the shortest diffusion delay employed for an adequate sampling of the decay curve on a typical high-resolution NMR probe. In addition, the maximum gain in efficiency is reached for $\Delta < T_1(^{15}N)$, which corresponds to typical diffusion delays Δ that yield sufficient absolute sensitivity.

Experimentally we compared the sensitivity of SORDID and BEST-XSTE by measuring diffusion rates of the H3-18 RNA kissing complex[18] and several globular proteins of different size: human ubiquitin, human Raf-1 Kinase Inhibitor Protein[19] (RKI protein, ^{13}C and ^{15}N labelled, 20 kDa, 187 residues), class B β-lactamase from *Bacillus cereus*[20] (BC2 protein, ^{15}N labelled, 25 kDa, 237 residues), and class A β-lactamase from *Bacillus licheniformis*[21] (BS3 protein, ^{15}N labelled, 30 kDa, 268 residues).

The results in Fig. 3 are qualitatively in agreement with theoretical estimates. However, the observed signal enhancements were systematically higher than expected. This can be explained by the use of shorter soft rectangular pulses and harder composite pulses in SORDID compared to BEST-XSTE, since the latter used selective RE-BURP (180°) and E-BURP (90°) pulses.[22] Replacing the shaped pulses of the BEST-XSTE sequence by rectangular pulses as in SORDID led surprisingly to gains that were about 10% less than expected. Because of the offset dependence of the effective tilt angle, a soft rectangular 90° pulse leaves more magnetization

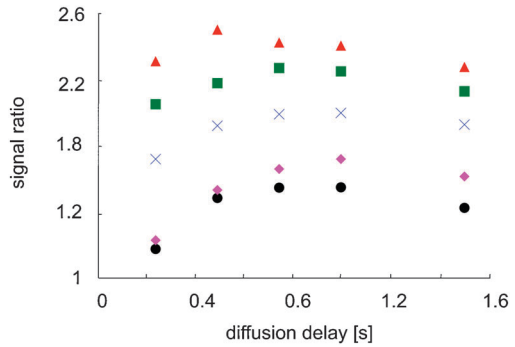

Fig. 3 Ratios of signal integrals obtained with SORDID and BEST-XSTE experiments for different diffusion delays Δ. Experiments were carried out for human ubiquitin (black circles, 8.6 kDa), RNA kissing complex (magenta diamonds, 9.5 kDa), RKI protein (blue crosses, 20 kDa), BS3 protein (green squares, 30 kDa), and BC2 protein (red triangles, 25 kDa). The data were obtained from 1D spectra measured with low diffusion gradient amplitudes ($G^i_{\mathrm{encode}} = G^i_{\mathrm{decode}} = 4.43$ G cm^{-1}). The recycle delay T_{RD} of BEST-XSTE experiments was optimized for each molecule. Experiments on proteins were all carried out at 293 K, those on RNA at 278 K. The measured average (standard deviation) diffusion constants were $D = 7.4\ (0.1) \times 10^{-11}$, $12.3\ (0.1) \times 10^{-11}$, $7.9\ (0.2) \times 10^{-11}$, $8.2\ (0.1) \times 10^{-11}$ and $4.4\ (0.4) \times 10^{-11}$ m^2 s^{-1} for BC2, ubiquitin, BS3, RKI and RNA, respectively.

along the z-axis, so that BEST-XSTE with soft rectangular 90° pulses will also benefit from improved recovery of longitudinal proton magnetization during the diffusion delay.

The measured values of the factor κ vary dramatically between ubiquitin in a low pH buffer ($\kappa_{\mathrm{ub}} = 2.8$) and BC2 and BS3 proteins ($\kappa_{\mathrm{BS3}} \approx \kappa_{\mathrm{BC2}} = 19$). As expected, the optimal diffusion delay decreases when κ increases, though somewhat less than expected. Relaxation properties in RNA, in particular cross-relaxation of imino and aromatic protons and chemical exchange with water protons, lead to the surprising result that, while κ is large ($\kappa_{\mathrm{RNA}} = 26$), the efficiency gain is comparable to ubiquitin. Nevertheless, the sensitivity improvement of SORDID is higher than any reported recently.[12,13] Moreover, setting up SORDID experiments is straightforward, since only a single parameter (Δ) needs to be optimized as opposed to two parameters (Δ and T_{RD}) in traditional schemes.

We thank Yannis Karsisiotis, Julie Vandenameele and Laurette Tavel (Université de Liège) for the preparation of BC2, BS3 and RKI protein samples as well as Chul-Hyun Kim (University of California at Davis) for the RNA kissing complex.

Notes and references

1 E. L. Hahn, *Phys. Rev.*, 1950, **80**, 580.
2 E. O. Stejskal and J. E. Tanner, *J. Chem. Phys.*, 1965, **42**, 288.
3 C. S. Johnson, *Prog. Nucl. Magn. Reson. Spectrosc.*, 1999, **34**, 203.
4 Y. Cohen, L. Avram and L. Frish, *Angew. Chem., Int. Ed.*, 2005, **44**, 520.
5 A. S. Altieri, D. P. Hinton and R. A. Byrd, *J. Am. Chem. Soc.*, 1995, **117**, 7566.
6 K. F. Morris and C. S. Johnson, *J. Am. Chem. Soc.*, 1992, **114**, 3139.
7 V. Y. Orekhov, D. M. Korzhnev, K. V. Pervushin, E. Hoffman and A. S. Arseniev, *J. Biomol. Struct. Dyn.*, 1999, **17**, 157.
8 W. Y. Choy, F. A. A. Mulder, K. A. Crowhurst, D. R. Muhandiram, I. S. Millett, S. Doniach, J. D. Forman-Kay and L. E. Kay, *J. Mol. Biol.*, 2002, **316**, 101.
9 F. Ferrage, M. Zoonens, D. E. Warschawski, J.-L. Popot and G. Bodenhausen, *J. Am. Chem. Soc.*, 2003, **125**, 2541.
10 F. Ferrage, M. Zoonens, D. E. Warschawski, J.-L. Popot and G. Bodenhausen, *J. Am. Chem. Soc.*, 2004, **126**, 5654.
11 P. Ahuja, R. Sarkar, P. R. Vasos and G. Bodenhausen, *J. Am. Chem. Soc.*, 2009, **131**, 7498.
12 R. Augustyniak, F. Ferrage, R. Paquin, O. Lequin and G. Bodenhausen, *J. Biomol. NMR*, 2011, **50**, 209.
13 R. Horst, A. L. Horwich and K. Wuthrich, *J. Am. Chem. Soc.*, 2011, **133**, 16354.
14 P. Schanda, H. Van Melckebeke and B. Brutscher, *J. Am. Chem. Soc.*, 2006, **128**, 9042.
15 R. Sarkar, D. Moskau, F. Ferrage, P. R. Vasos and G. Bodenhausen, *J. Magn. Reson.*, 2008, **193**, 110.
16 J. Simbrunner and G. Zieger, *J. Magn. Reson., Ser. B*, 1995, **106**, 142.
17 G. A. Morris and R. Freeman, *J. Am. Chem. Soc.*, 1979, **101**, 760.
18 C. H. Kim and I. Tinoco, *Proc. Natl. Acad. Sci. U. S. A.*, 2000, **97**, 9396.
19 S. Huerta-Yepez, N. K. Yoon, A. Hernandez-Cueto, V. Mah, C. M. Rivera-Pazos, D. Chatterjee, M. I. Vega, E. L. Maresh, S. Horvath, D. Chia, B. Bonavida and L. Goodglick, *BMC Cancer*, 2011, **11**, 259.
20 L. I. Llarrull, M. F. Tioni and A. J. Vila, *J. Am. Chem. Soc.*, 2008, **130**, 15842.
21 E. Sauvage, A. Zervosen, G. Dive, R. Herman, A. Amoroso, B. Joris, E. Fonze, R. F. Pratt, A. Luxen, P. Charlier and F. Kerff, *J. Am. Chem. Soc.*, 2009, **131**, 15262.
22 H. Geen and R. Freeman, *J. Magn. Reson.*, 1991, **93**, 93.